Underwater Wide-Field Tomography of Sediment Resuspension

Adi Vainiger [1], Yoav Y. Schechner [1], Tali Treibitz [2], Aviad Avni [2] , David S. Timor[3]

[1] Viterbi Faculty of Electrical Engineering, Technion - Israel Institute of Technology, Haifa, Israel.

[2] Leon H. Charney School of Marine Sciences - University of Haifa, Israel. [3] Ha-Aliya Street 38, Nesher , Israel

adi.vainiger@gmail.com; yoav@ee.technion.ac.il ; ttreibitz@univ.haifa.ac.il; aavni@univ.haifa.ac.il;

Sediment resuspension affects physical, chemical and biological processes in the sea [1-3]. Biological sediment resuspension, caused by activity of benthic fish is common [4]. These events are temporally abrupt and spatially discrete. Understanding resuspension requires a wide set of methods [5-9]. Existing in-situ methods quantify sediment resuspension in cm-scale [10-16]. We seek multi-meter-scale measurements of these events using far-field cameras. We develop an imaging technology designed to (a) observe the seafloor and the water medium above it from a distance, (b) sense sediment resuspension events, and (c) algorithmically quantify the resuspension.

Our technology quantifies the amount of material lifted, and its spatio-temporal distribution. The spatial distribution of the particles is three-dimensional (3D). Hence, we develop an imaging system to reconstruct sediment resuspension in 3D. To achieve this, the evolving sediment plume is imaged against a diffuse backlight. Imaging is done simultaneously from multiple directions (Fig. 1[Left]). The resuspended particles affect light that reaches the cameras. Analysis uses a computed tomography (CT) principle [17-20]. Medical CT, as a means for volumetric sensing, motivates this. Underwater imaging is challenging [21-24]. Refractions and reflections complicate imaging even in controlled lab settings. Moreover, a large

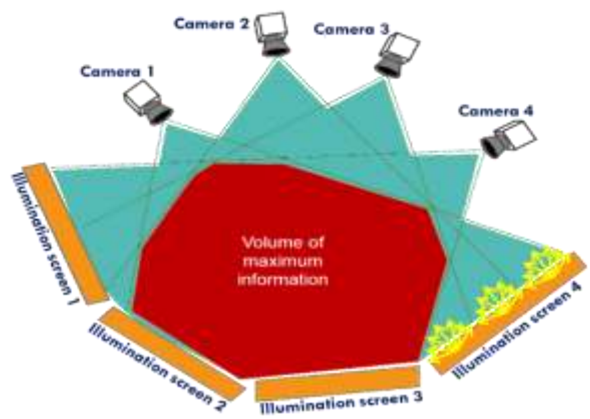

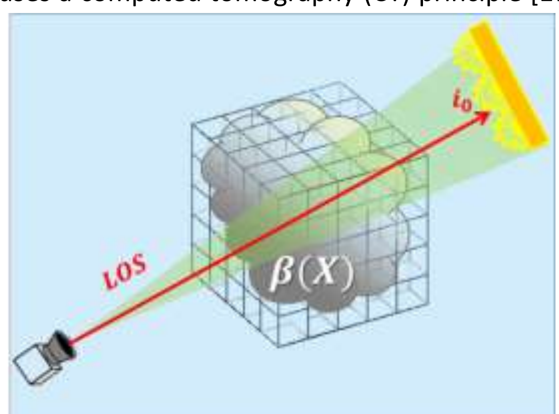

Figure 1: [Left] Illustration of tomographic system. [Right] LOS of a pixel.

submerged system affects flow and consequently may bias measurements. Therefore, we develop optical and algorithmic techniques, aiming to reduce as much as possible these obstacles.

Let a screen have radiance i_0. Pixel p in a camera senses the radiance along a line of sight (LOS), as shown

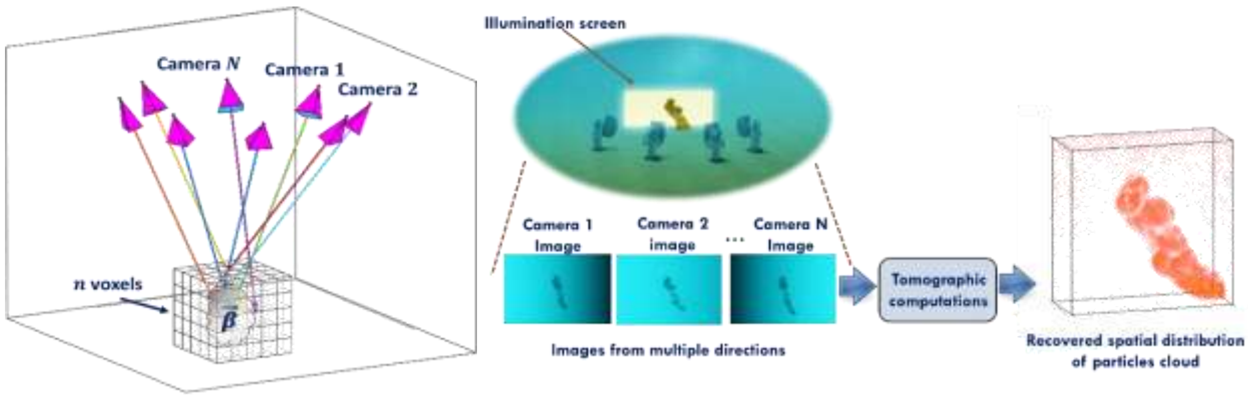

Figure 2: [Left] Projections from n voxels to m pixels. [Right] Flow of simulations environment.

Fig. 1[Right]. Particles in the medium have extinction cross section σ. The extinction coefficient is $\beta = \sigma\rho$, where ρ is the particles' density. The optical depth on the LOS is

$$\tau = \int_{\mathrm{LOS}} \beta(r)dr. \tag{1}$$

The transmitted radiance is

$$i = i_0 e^{-\tau}. \tag{2}$$

Let β^{Water}, $\beta(r)^{\mathrm{Sediment}}$ be the extinction coefficients of water and sediment particles, respectively. The radiance reaching pixel p through sediment-free water is $i_p^{\mathrm{W}} \triangleq i_0 e^{-\int_{\mathrm{LOS}} \beta^{\mathrm{Water}} dr}$. Then, the radiance through the resuspension is

$$i_p = i_p^{\mathrm{W}} e^{-\int_{\mathrm{LOS}} \beta(r)^{\mathrm{Sediment}} dr}. \tag{3}$$

Hence, the optical depth is

$$\tau_p = -\ln\left(\frac{i_p}{i_p^{\mathrm{W}}}\right) = \int_{\mathrm{LOS}} \beta(r)^{\mathrm{Sediment}} dr. \tag{4}$$

Tomographic setups have multidirectional LOSs through the scene (Fig. 2[left]). From Eq. (4),

$$\tau_{\mathrm{p}} \approx \sum_v a_{p,v} \beta_v^{\mathrm{Sediment}} \triangleq \vec{a}_p \vec{\beta}^{\mathrm{Sediment}}, \tag{5}$$

where $a_{p,v}$ is the length of the ray segment in the LOS of pixel p, in voxel v. Here $\beta_v^{\mathrm{Sediment}}$ is the sediment extinction coefficient of voxel v. Let $\vec{\beta}^{\mathrm{Sediment}} \epsilon \mathbb{R}^{n\times 1}$ represent the volumetric extinction coefficients in all voxels $v \in 1..n$. The overall sampled data is $\vec{\tau} \in \mathbb{R}^{m\times 1}$ representing sampled optical depths in each pixel $p \in 1..m$. Then,

$$\vec{\tau} \approx A\vec{\beta}^{\mathrm{Sediment}}. \tag{6}$$

Here $A \in \mathbb{R}^{m \times n}$ is a projection matrix. The volumetric extinction coefficient is estimated by

$$\hat{\beta} = argmin\|A\vec{\beta} - \vec{\tau}\|_2^2. \tag{7}$$

We tested this concept using both simulations and experiments. Physics based rendering [25-27] synthetically simulates underwater imaging. The simulation analyzes the rendered images and performs 3D tomographic reconstruction. This enables optimization of the system. Simulations (Fig. 2[Right]) show successful reconstruction of synthetic clouds. We performed experiments in a research seawater pool. The optical system contained eight sealed cameras, directed to the volume of interest above a lighting screen (Fig. 3). We externally controlled the cameras to simultaneously image the scene from several perspectives. We used openCV [28], a calibration board, markers on the screen and Agisoft [29], to calibrate the system geometry. This led us to the projection matrix A used in Eqs. (6,7). Before each resuspension event, we imaged the lighting screen. Inspired by the *communicating vessels principle*, we built an injection system. A bucket contained MP SILICA $12-26[um]$ particles suspended in water at density of $22.5\ [gr/l]$. Two liters were drained within ~ 63 sec, to shoot a resuspended cloud from the middle of the lighting screen. Resuspension was imaged at 10 fps.

Fig. 4[Left] shows two viewpoints: without sediment $\left(I^{\mathrm{W}}\right)$, then a resuspension event and finally the sediment optical depth. We used AIRtool [30] for Simultaneous Algebraic Reconstruction Technique

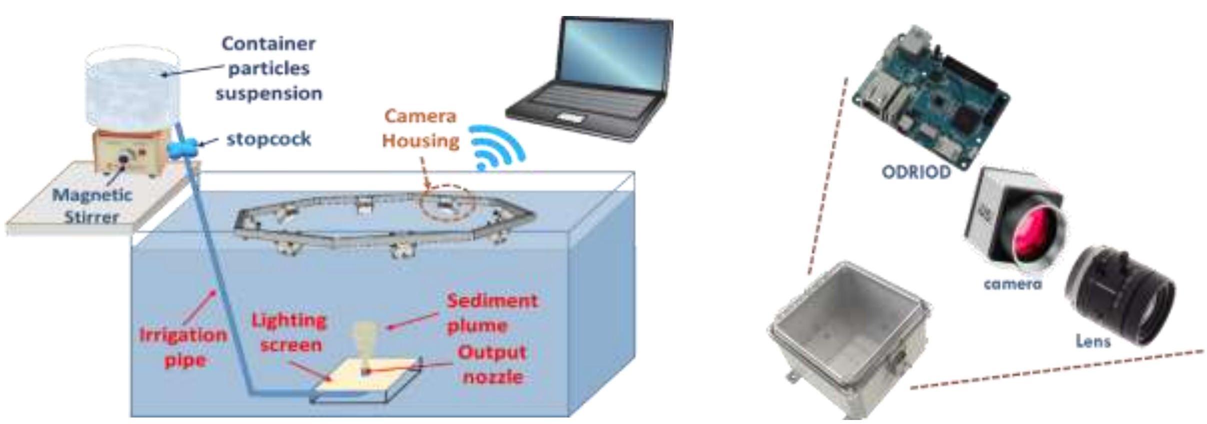

Figure 3: [Left] Camera housings are mounted on an octagonal frame. The frame resides ~2.5[m] above the lighting screen. From middle of lighting screen, emerges an output nozzle. [Right]Each housing contains an ODRIOD XU-4, an IDS UI-3260 camera, and a Tamron M112FM12 lens Figure

(SART) [31] in the tomography analysis. Fig. 4[Right] shows a meter-scale recovery of the sediment cloud (green channel), in $2[cm]$ voxel resolution.

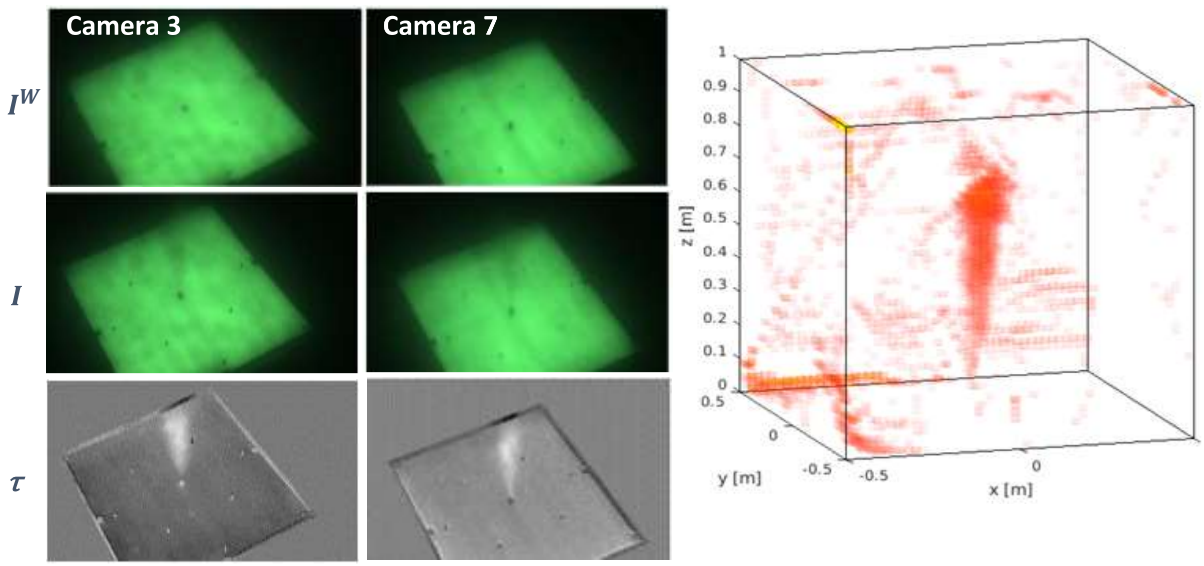

Figure 4: [Left] top - Background images (I^W), middle - Sediment cloud images (I), bottom - Optical depth images(τ) .[Right] Sediment cloud 3D recovery.

We envision future developments to obviate active lighting in tomographic setups. Such a system may enable research of marine animals which create resuspension events. The system can advance other underwater imaging applications.

We thank M. Fisher, Y. Goldfracht, L. Dehter, B. Herzberg, A. Levy , J. Fischer, S. Cohen, M. Groper, S. Farber for assisting in system construction and experiments. We thank V. Holodovsky, A. Levis, A. Aides, T. Katz, U. Shavit, G. Yahel, S. Grossbard for fruitful discussions, and I. Talmon J. Erez for technical support. YYS is a Landau Fellow - supported by the Taub Foundation and Israeli Ministry of Science, Technology and Space (Grant 3-12478). His work is conducted in the Ollendorff Minerva Center. Minerva is funded through the BMBF. TT is supported by The Leona M. and Harry B. Helmsley Charitable Trust and The Maurice Hatter Foundation.

References

Valeur JR, Jensen A, Pejrup M. Turbidity, particle fluxes and mineralisation of carbon and nitrogen in a shallow coastal area. Marine and freshwater research. 1995;46(1):409-18.

Tengberg A, Almroth E, Hall P. Resuspension and its effects on organic carbon recycling and nutrient exchange in coastal sediments: in situ measurements using new experimental technology. Journal of Experimental Marine Biology and Ecology. 2003;285:119-42.

Wainright SC. Stimulation of heterotrophic micro plankton production by resuspended marine sediments. Science. 1987;238(4834):1710-2.

Katz T, Yahel G, Reidenbach M, Tunnicliffe V, Herut B, Crusius J, Whitney F, Snelgrove PV, Lazar B, Resuspension by fish facilitates the transport and redistribution of coastal sediments. Limnology and Oceanography. 1;57(4):945-58.

Yahel G, Yahel R, Katz T, Lazar B, Herut B, Tunnicliffe V, Fish activity: a major mechanism for sediment resuspension and organic matter remineralization in coastal marine sediments. Marine Ecology Progress Series. 2008;372:195-209.

Shavit U, Halamish A, Grossbard S, Asher S, Gilboa M, Katz T, Yahel G, Testing a biological resuspension footprint model using Lagrangian simulations. PiE 2018.

Grossbard S, Gilboa M., Katz T, Yahel G., Shavit U, Developing a laboratory simulator for the study of resuspension events. PiE 2018.

Gilboa M, Katz T, Shavit U, Grosbard S , Torfstien Adi, Yahel G, Novel approach to measure the rate of sediment resuspension at the ocean and to estimate the contribution of fish activity to this process. PiE 2018.

Yahel G, Gilboa M, Grossbard S, Vainiger A, Treibitz T, Schechner Y, Shavit U, Katz T, Biological activity: an overlooked, mechanism for sediment resuspension, transport, and modification in the ocean. PiE 2018.

Raffel M, Willert CE, Scarano F, Kähler CJ, Wereley ST, Kompenhans J., *Particle image velocimetry: a practical guide*. Springer; 2018.

Elsinga GE, Scarano F, Wieneke B, van Oudheusden BW., Tomographic particle image velocimetry. Experiments in fluids. 2006;41(6):933-47.

Klinner J, Willert C. Tomographic shadowgraphy for three-dimensional reconstruction of instantaneous spray distributions. Experiments in fluids. 2012;53(2):531-43.

Shahi S, Kuru E., An experimental investigation of settling velocity of natural sands in water using Particle Image Shadowgraph. Powder Technology. 2015 ;281:184-92.

Thompson CE, Couceiro F, Fones GR, Helsby R, Amos CL, Black K, Parker ER, Greenwood N, Statham PJ, Kelly-Gerreyn BA., In situ flume measurements of resuspension in the North Sea. Estuarine, Coastal and Shelf Science. 2011;94(1):77-88.

Fugate DC, Friedrichs CT. Determining concentration and fall velocity of estuarine particle populations using ADV, OBS and LISST. Continental Shelf Res.2002;22(11-13):1867-86.

Ochiai S, Kashiwaya K., Measurement of suspended sediment for model experiments using general-purpose optical sensors. Catena. 2010;83(1):1-6.

Aides A, Schechner YY, Holodovsky V, Garay MJ, Davis AB. Multi sky-view 3D aerosol distribution recovery. Optics Express. 2013 ;21(22):25820-33.

Alterman M, Schechner YY, Vo M, Narasimhan SG. Passive tomography of turbulence strength. In European Conference on Computer Vision 2014 pp. 47-60. Springer.

Holodovsky V, Schechner YY, Levin A, Levis A, Aides A, In-situ multi-view multi-scattering stochastic tomography. Proc. IEEE Int. Conf. Computational Photography 2016.

Levis A, Schechner YY, Talmon R. Statistical tomography of microscopic life. Proc. IEEE Computer Vision and Pattern Recognition 2018 pp. 6411-6420.

Treibitz T, Schechner YY. Turbid scene enhancement using multi-directional illumination fusion. IEEE Transactions on Image Processing. 2012;21(11):4662-7.

Treibitz T, Schechner Y, Kunz C, Singh H., Flat refractive geometry. IEEE transactions on pattern analysis and machine intelligence. 2012;34(1):51-65.

Schechner YY, Karpel N., Attenuating natural flicker patterns. Proc. MTS/IEEE OCEAN 2004, Vol. 3, pp. 1262-1268.

Sheinin M, Schechner YY., The next best underwater view. Proc. IEEE Computer Vision and Pattern Recognition 2016 pp. 3764-3773.

Pharr M, Jakob W, Humphreys G., *Physically based rendering: From theory to implementation.* Morgan Kaufmann; 2016.

Narasimhan SG, Gupta M, Donner C, Ramamoorthi R, Nayar SK, Jensen HW., Acquiring scattering properties of participating media by dilution. In ACM TOG 2006 Vol. 25, No. 3, pp. 1003-1012.

Mobley CD. *Light and water: radiative transfer in natural waters.* Academic press; 1994.

https://pypi.org/project/opencv-python/

http://www.agisoft.com/pdf/photoscan-pro_1_4_en.pdf

http://www2.compute.dtu.dk/~pcha/AIRtoolsII/AIRtoolsManual.pdf

Andersen AH, Kak AC., Simultaneous algebraic reconstruction technique (SART): a superior implementation of the ART algorithm. Ultrasonic Imaging. 1984;6(1):81-94.